# Structure of Mn films grown on (111) and (001) fcc Ir determined by EXAFS and the multiple-scattering approach

S. Andrieu, H. M. Fischer, and M. Piecuch
*Laboratoire de Métallurgie Physique et Sciences des Matériaux, CNRS/Université Henri Poincaré de Nancy, Boîte Postale 239, 54506 Vandoeuvre, France*

A. Traverse
*Laboratoire pour l'Utilisation du Rayonnement Synchrotron, CNRS/CEA/Université Paris sud, 91405 Orsay, France*

J. Mimault
*Laboratoire de Métallurgie Physique, CNRS/Université de Poitiers, 86022 Poitiers, France*
(Received 14 February 1996)

Mn films were grown on (001) and (111) fcc Ir lattices by molecular beam epitaxy, extended x-ray absorption fine structure (EXAFS) experiments were performed on these films in order to determine the Mn structures. As Mn can adopt different crystalline structures, it is first shown that the usual Fourier treatment of EXAFS oscillations is not an appropriate technique for this purpose. On the contrary, the application of multiple scattering theory of x-ray-absorption fine structure allows us to identify the structures. For relaxed (polycrystalline) thick Mn deposits, Mn crystallizes in the Mn$\alpha$ structure. For unrelaxed (single-crystalline) thick Mn films, the Mn EXAFS oscillations are well simulated assuming a mixing of fcc and Mn$\alpha$ structure. For thin Mn films in Mn/Ir (111) and (001) superlattices, this multiple scattering approach allows us to show that Mn is in a trigonal structure when it is grown on Ir(111) and a tetragonal structure when it is grown on Ir(001). Finally, the $(\sqrt{3}\times\sqrt{3})R30°$ superstructure of Mn films grown on (111) Ir is shown to come from the epitaxy of a mixed fcc and Mn$\alpha$ structures and not from the occurence of Mn Laves phases like $Cu_2Mg$ or $Zn_2Mg$ as assumed by several workers. [S0163-1829(96)10827-4]

## I. INTRODUCTION

The interrelation between structure and magnetic properties of transition metals has recently recovered a great deal of interest with the possibility to grow artificial structures. By means of molecular-beam-epitaxy (MBE) technique, metals with unusual, otherwise unstable, crystallographic structures can actually be grown by epitaxy. The general purpose of our work is thus to prepare transition metals of the first series in new crystalline structures to determine these structures.

The structure of the deposited metal $M$ depends on the structure of the substrate or buffer layer $X$ used. Consequently, a large number of $MX$ system have been studied.[1,3] In our group, such an approach was previously used for Fe grown on (0001) Ru, (111) Ir, and (001) Ir.[2,3] For these systems, the Fe crystalline structure was rather easy to determine by using standard techniques like x-ray diffraction (XRD) and electron diffraction,[2,3] because the standard Fe structures (fcc, bcc, hcp) are fairly simple. In the case of Mn, the situation is more involved. First, the Mn structure in the normal conditions of temperature and pressure is a complex structure, usually called Mn$\alpha$, which contains 58 atoms in the primitive cell.[4] For higher temperatures, Mn is stabilized in a second complex structure, usually called Mn$\beta$, which contains 20 atoms in the primitive cell.[4] Consequently, it is possible to obtain a complex structure in a Mn film, even when it is grown on a simple surface lattice. For instance, it is well known that the surface structure of a Mn film grown on a hexagonal lattice is a $(\sqrt{3}\times\sqrt{3})R30°$ superstructure. This superstructure can arise from a surface atom arrangement due to the two-dimensional scale of the surface lattice, but can also be due to a three-dimensional arrangement of the atoms in the entire Mn film. This superstructure can actually be explained by the occurrence of a Mn Laves phase like $Cu_2Mg$ or $Zn_2Mg$ as proposed by Heinrich *et al.*[5] The determination of the structure is thus only possible by an intensity analysis of the corresponding electron or XRD diagrams. Concerning electron diffraction, such a quantitative analysis is difficult when the structure is complex. The modeling of XRD diagrams obtained on thick films is simpler. However, the critical thickness of the Mn films grown on Ir buffer layers is small. Superlattices (SL's) have thus to be grown in order to have a sufficient amount of materials for diffraction measurements performed on a regular apparatus. In that case, the structural form factor is a complex combination of the structural form factors of Mn and Ir.[6] It thus becomes very difficult to determine the structure of Mn in SL's. Up to now, the electron diffraction and XRD techniques available in our laboratory do not allow us to clearly identify the structure of Mn films deposited on Ir.

Another possibility to obtain structural information is to perform extended x-ray absorption fine structure (EXAFS) experiments. We always use this technique, even for the study of rather simple structures, like body-centered tetragonal Fe structure on (001) Ir,[7] because the determination of the Fe structure based on XRD is not direct. Indeed, an average (001) distance [equal to a linear combination of the (001) distances in Fe and Ir layers] is obtained with XRD. In the case of EXAFS experiments, this problem of average structural information does not exist since it is an element

 

selective technique. In the case of Mn, this EXAFS technique is now essential in order to determine the structure. This work is thus dedicated to the structure determination of Mn films deposited on (111) and (001) Ir using polarized EXAFS. Indeed, additional structural information can be obtained by applying the linear polarization of the x-ray beam in and out of the film's plane. The standard Fourier treatment of the EXAFS oscillations is first applied. However, we show that this determination of the first-neighbor distance and coordination numbers is not sufficient to determine the structure of the Mn films. We thus apply the multiple-scattering theory to EXAFS (Ref. 8) in order to obtain more complete information.

## II. EXPERIMENTS

### A. Sample preparation

The Mn films were grown in a MBE chamber with a residual vacuum around $5\times10^{-11}$ torr. The (111) Mn/Ir SL's were grown at 400 K on a (111) Ir buffer layer grown on (1120) sapphire substrates. The (001) Mn/Ir SL's were also grown at 400 K but on a (001) Ir buffer layer grown on (001) MgO substrates. The details of the substrate and buffer preparation are given in Refs. 2 and 3. Ir was evaporated using an electron gun at a growth rate of 0.5 Å/s and Mn was sublimated by using a Knudsen cell heated up to 1200 K. The resulting growth rate is around 0.1 Å/s. The residual pressure in the chamber during the growth was not higher than $10^{-10}$ torr, which avoids any carbon and oxygen contamination. This was controlled by Auger electron spectroscopy. The thicknesses of Mn and Ir layers in SL's were varied from 2 to 30 Å. Thick Mn films were also grown in order to study the structural relaxation of the Mn films as a function of their thickness. The Mn and Ir growth was controlled by reflexion high energy electron diffraction (RHEED). The variation of the in-plane distance was also determined by RHEED, and the out-of-plane distance was determined using XRD in the $\theta$-$2\theta$ mode. The thick films and SL's were always grown at 400 K. A detailed description of the Mn/Ir sample preparation and analysis is given in Refs. 9 and 10.

### B. Growth results

*Mn on (111) Ir*. For Mn thickness up to 3 ML, the Mn surface structure is pseudomorphic to the hexagonal Ir surface lattice as shown by RHEED. Above 3 ML, a $(\sqrt{3}\times\sqrt{3})$R30° superstructure is observed and is maintained up to a thickness of around 100 Å. Above this critical thickness, complex RHEED patterns with a large number of diffracted spots very close to one another are observed. XRD experiments show that for Mn layer thicknesses below 30 Å, the Mn interlayer distance is around 2.15 Å.

*Mn on (001) Ir*. For Mn films up to 100 Å thick, the Mn surface structure is pseudomorphic to the initial $1\times1$ Ir square surface lattice. The in plane distance varies from the (200) Ir distance (1.92 Å) to 1.8 Å for thick Mn films. The out-of-plane distance is around 1.8 Å as shown by XRD experiments. Above 100 Å thickness, a complex RHEED pattern similar to those observed on (111) Ir takes place.

All the details of these results are given in Ref. 9. The flatness of the SL's interfaces and the lack of interdiffusion are checked by transmission electron microscopy and off-specular diffraction experiments.[10]

According to these growth observations, specific samples were prepared in order to analyze the corresponding Mn structure by EXAFS.

(i) Relaxed thick Mn films grown on (111) and (001) Ir: the thickness of the films was about 350 Å. The RHEED pattern at the end of the Mn growth was complex.

(ii) Unrelaxed thick Mn films grown on (111) and (001) Ir: the thickness of the films was around 100 Å. At the end of the growth, a Mn $(\sqrt{3}\times\sqrt{3})$R30° surface structure was observed on (111) Ir and a Mn $1\times1$ surface structure was observed on (001) Ir.

TABLE I. Space groups, parameters, atom positions, and atomic volumes for the six structures used to calculate the EXAFS spectra with FEFF6 code (Ref. 8).

| Structure | Space group | Parameters (Å) | Atom positions and number of atom per cell | | | | Volume (Å$^3$/atom) |
|---|---|---|---|---|---|---|---|
| Mn $\alpha$ | $I\bar{4}3m$ | $a=8.914$ | 0 | 0 | 0 | (2) | 12.21 |
| | | | 0.317 | 0.317 | 0.317 | (8) | |
| | | | 0.356 | 0.356 | 0.042 | (24) | |
| | | | 0.089 | 0.089 | 0.278 | (24) | |
| Mn $\beta$ | $P4_132$ | $a=6.315$ | 0.0636 | 0.0636 | 0.0636 | (8) | 12.59 |
| | | | 0.125 | 0.2022 | 0.4522 | (12) | |
| Laves phase ($Cu_2Mg$) | $Fd3m$ | $a=6.651$ | 0.625 | 0.625 | 0.625 | (16) | 12.25 |
| | | | 0 | 0 | 0 | (8) | |
| Laves phase ($Zn_2Mg$) | $P63/_mmc$ | $a=4.703$ | 0 | 0 | 0 | (2) | 12.32 |
| | | | 0.3333 | 0.6667 | 0.0629 | (4) | |
| | | $c=7.717$ | 0.8305 | 0.660 | 0.250 | (6) | |
| fcc | $Fm3m$ | $a=3.84$ | 0 | 0 | 0 | (4) | 14.16 |
| bcc | $Im3m$ | $a=2.715$ | 0 | 0 | 0 | (2) | 10.01 |

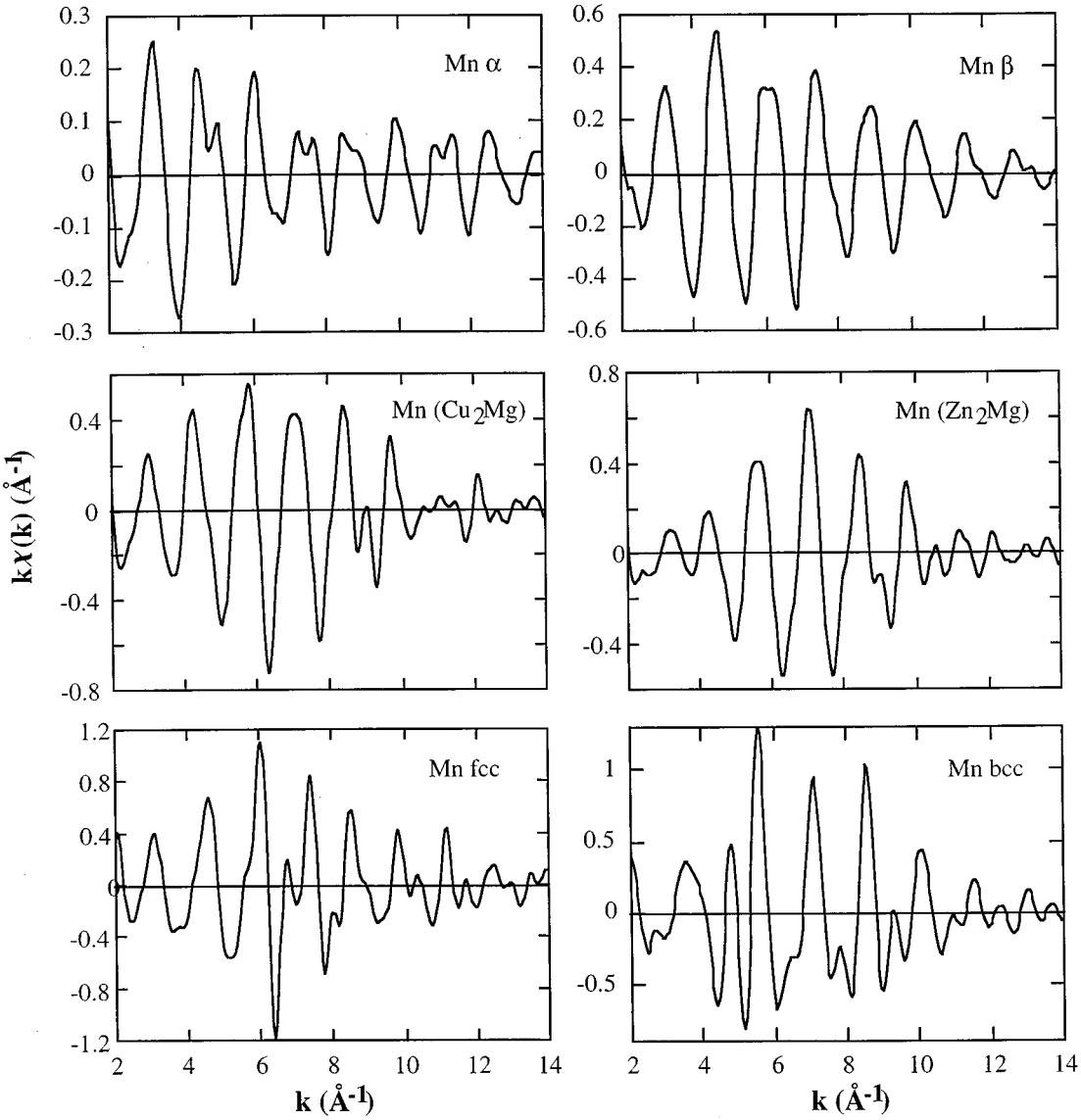


FIG. 1. Calculated EXAFS oscillations using the multiple scattering theory for the six structures defined in Table I. The calculations were performed with a randomly oriented polarization. It is worth noticing that the spectra are very different from one structure to another.

(iii) Mn/Ir(111) SL's: the Mn layers were 15 Å thick and the Ir layers thickness was varied from 2 to 20 Å. At the end of the Mn growth, a Mn $(\sqrt{3}\times\sqrt{3})$R30° surface structure was observed. A 1×1 surface structure was observed during the Ir growth.

(iv) Mn/Ir(001) SL's: the Mn layers were 10 and 20 Å thick and the Ir layers thickness was varied from 2 to 20 Å. A 1×1 surface structure was observed during the Ir and Mn growth.

### C. EXAFS measurements and data analysis

Data collection was carried out at liquid-nitrogen temperature (details of the detector described in Ref. 11) on the D42 station of the DCI storage ring in the Laboratoire pour l'Utilisation du Rayonnement Electromagnétique (LURE) at the Mn *k*-edge (6545 eV) using a Si (331) channel-cut monochromator. Measurements were performed in the reflection mode and the total electron yield was used as the sample depth is compatible with SL's thicknesses (about 700 Å for an energy of 7 keV). The measurements were performed using two geometries, i.e., with the sample oriented parallel or perpendicular to the direction of the x-ray beam polarization vector. The x-ray absorption spectroscopy spectra were recorded from 6510 to 6630 eV with 0.5-eV steps in the x-ray absorption near-edge structure (XANES) region and from 6500 to 7300 eV with 2-eV steps in the EXAFS region. The EXAFS oscillations were extracted using standard method.[12] The background was substracted using a polynomial function, and normalized to the height of the absorption step edge. The origin of the energy scale was fixed at 6545 eV. The experimental EXAFS oscillations were analyzed in two different ways: either they were treated using the standard procedure or they were compared to calculated spectra using the multiple scattering (MS) method.[8]

In the first case, the EXAFS oscillations were Fourier transformed in the range 2.5–14 Å.[1] This large range is due to the low-temperature measurements. The fit of the first peak of the Fourier transform was done using the phase and amplitudes of Co calculated with the McKale's code.[13]

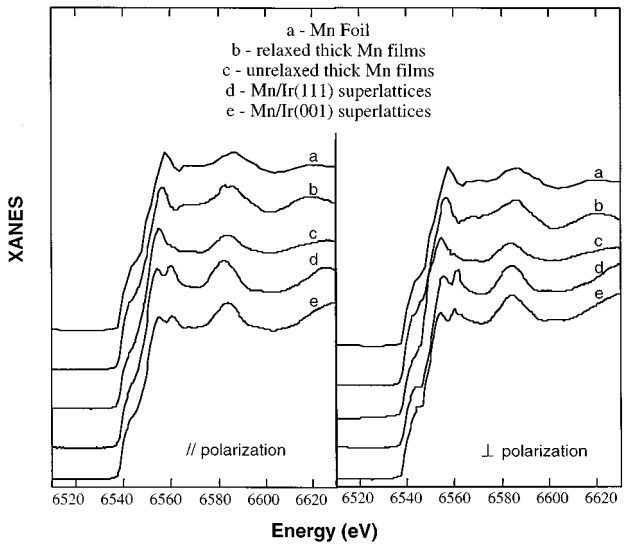


FIG. 2. XANES spectra for a Mn$\alpha$ foil and the four kinds of samples with in- and out-of-plane polarizations.

In the second case, the EXAFS oscillations were calculated using the FEFF6.01 code developed by Rehr and co-workers[8] to account for single- and multiple-scattering processes. The calculated EXAFS oscillations were thus simply compared to the experimental ones. In the simulations, only the structural parameters were varied. The amplitude reduction factor $S_0^2$ was always fixed to 1. The cluster size was chosen equal to the maximum possible value according to the structure. At this stage of investigations, it is however necessary to verify that the simulated EXAFS spectra are actually very different for the different Mn possible structures. Since Mn can exist in Mn$\alpha$, Mn$\beta$, fcc, and bcc structures, it is necessary to simulate the EXAFS oscillations for these structures. Moreover, several workers[5,14] also proposed that Mn can be stabilized in $Cu_2Mg$ or $Zn_2Mg$ Laves phases on hexagonal surface lattices. Therefore, it is necessary to calculate the EXAFS oscillations for these six structures, and to compare the results in order to determine if it is possible to decide between them. Moreover, we know that the in-plane parameter is equal to the Ir parameter for unrelaxed thick films or for SL's, as shown by RHEED. Consequently, the in-plane parameter has to be chosen equal to the Ir parameter in order to have a coherent growth of these phases on the initial Ir (111) or (001) lattices. It is thus necessary to know how the assumed Mn structure matches the Ir (100) or (111) lattices. In this first approach, unstrained structures are taken into account. This is sufficient to decide if whether or not the EXAFS oscillations are different from one structure to another.

The following epitaxial relation are used in this study.

(i) fcc and bcc Mn growth: as the fcc and bcc structures are cubic, the (001) planes of fcc or bcc Mn can match the (001) Ir lattice. The (100) parameter of fcc Mn structure is thus chosen equal to the bulk fcc (100) Ir parameter, and the (100) parameter of bcc Mn structure is chosen equal to the bulk fcc (110) Ir parameter. This fcc Mn structure can also be grown on (111) Ir lattice.

(ii) Laves phases growth: the matching of Laves phases on the (111) Ir lattice is not so simple. Heinrich *et al.*[5] explained in a subtle and satisfactory way how the $Cu_2Mg$ or $Zn_2Mg$ Laves phases can be grown on (0001) Ru lattice to give a $(\sqrt{3}\times\sqrt{3})$R30° superstructure. Using their explanations, it is simple to determine that for the cubic $Cu_2Mg$ Lave phase, the (100) parameter has to be equal to three times the (111) Ir distance. For the hexagonal $Zn_2Mg$ Laves phase, the (100) parameter has to be equal to three times the (112) Ir distance. The (001) parameter is thus calculated using the $c/a$ ratio of the $Zn_2Mg$ Laves phase ($=1.641$).

(iii) Mn$\alpha$ and Mn$\beta$ growth: in this approach, these structures are taken into account to test the structure of relaxed thick Mn films. No epitaxial relation is thus necessary here. The corresponding EXAFS spectra are thus simulated using the standard parameter of these structures.

The space group, parameters, atom positions, and atomic volumes corresponding to these structures for which the EXAFS oscillations are calculated, are listed in Table I. It should be noted that the atomic volume of the arbitrary Mn Laves phases is consistent with the atomic volume of the existing Mn$\alpha$ and Mn$\beta$ structures. In this approach, the calculation of EXAFS oscillations was performed with a randomly oriented polarization.

The calculated EXAFS oscillations for these six structures are shown in Fig. 1. It is to be noticed that these spectra are very different from one structure to another. This means that the comparison of EXAFS oscillations is a powerful tool to determine the structure, even for similar structures like Mn$\alpha$, Mn$\beta$, and Laves phase structures.

## III. RESULTS

### A. Experimental XANES and EXAFS spectra

Typical XANES spectra observed for the four series of samples are displayed in Fig. 2. These spectra were compared to the XANES spectra obtained on a Mn$\alpha$ foil. First, it is possible to notice that these spectra are similar for in-plane and out-of-plane polarization. The XANES spectra measured on SL's (111) and (001) are similar and are typically the same as XANES spectra obtained on fcc or hcp materials. The XANES spectra of the relaxed thick Mn film are similar to the XANES spectrum obtained on the Mn$\alpha$ foil. Finally, the XANES spectra obtained on unrelaxed thick films is different from the others, although it does not differ too much from the Mn$\alpha$ XANES spectrum.

Again, typical EXAFS oscillations were observed for the four series of samples as shown in Fig. 3. A major difference can again be noticed between thick Mn films and SL's, i.e., the number of first neighbors is small in thick films since the maximum of $k\chi(k)$ never exceeds 0.35 $\text{Å}^{-1}$, whereas it is large in SL's since the maximum of $k\chi(k)$ can reach 1 $\text{Å}^{-1}$. This is consistent with XANES results. Moreover, additional information on the structure can be obtained by examining the EXAFS spectra for both $\parallel$ and $\perp$ polarizations. On the one hand, the observation of identical EXAFS spectra for both polarizations means that the film is in a polycrystalline state, or that the film is single crystalline but in a cubic structure. This is the case for thick Mn films (Fig. 3). On the other hand, the occurrence of different EXAFS spectra for both polarizations means that the film is in a single-crystalline state and that the film is not in a cubic phase. This is the case for superlattices (Fig. 3). Moreover, the RHEED observations allow us to go further. Indeed, complex

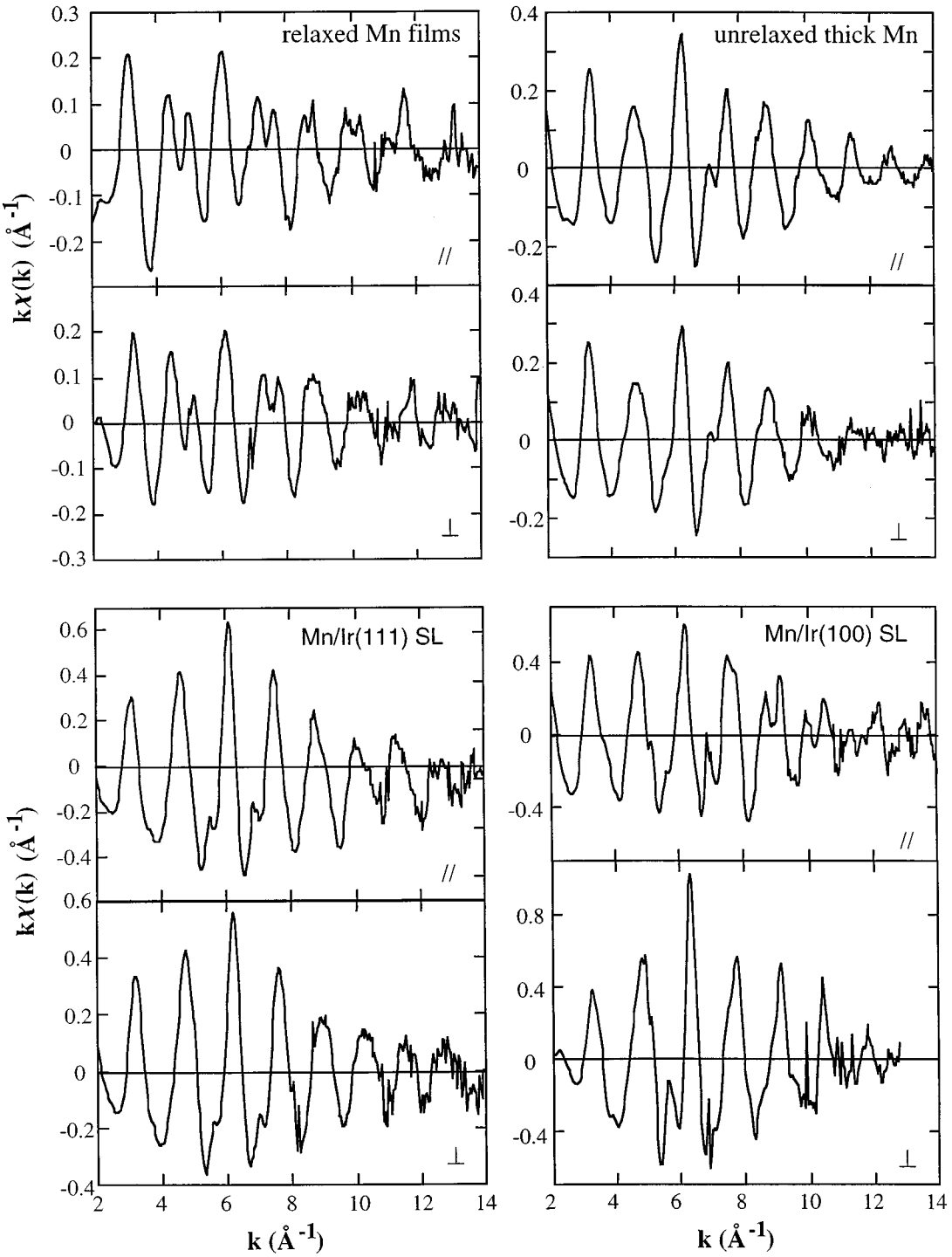


FIG. 3. Experimental EXAFS oscillations for the four kinds of samples with in- and out-of-plane polarizations.

RHEED patterns typical of a polycrystalline state were observed on relaxed thick Mn films. On the contrary, RHEED patterns typical of a single-crystalline state were observed on unrelaxed thick Mn films and on (111) and (001) SL's. According to RHEED and EXAFS observations, we conclude that (i) relaxed thick Mn films are polycrystalline, (ii) unrelaxed thick Mn films are single crystalline with a cubic structure, and (iii) (111) and (001) SL's are single crystalline with a noncubic structure.

### B. Standard EXAFS analysis

The standard EXAFS analysis applied on the four kinds of samples allows us to determine the first-neighbor distance and the corresponding coordination numbers. The results are listed in Table II. It appears that the predominant neighbor distance, which varies from 2.62 to 2.72 Å, is similar for all the samples. Another neighbor distance must be taken into account in order to correctly fit the data measured on relaxed thick films, i.e., 2.35 Å in parallel polarization and 3 Å in

TABLE II. First- and second-neighbor distances and coordination numbers for the four series of samples determined by using the standard EXAFS analysis.

| | 1st distance (Å) | | 2nd distance (Å) | | Number of neighbors | | | |
|---|---|---|---|---|---|---|---|---|
| Polarization | ∥ | ⊥ | ∥ | ⊥ | ∥ | ⊥ | ∥ | ⊥ |
| Relaxed thick films | 2.65 | 2.72 | 2.35 | 2.9 | 5.5 | 4.5 | 1.5 | 2 |
| Unrelaxed thick films | 2.69 | 2.67 | | 2.35 | 7 | 7 | | |
| Mn/Ir (111) SL's | 2.68 | 2.64 | | | 13 | 10 | | |
| Mn/Ir (001) SL's | 2.65 | 2.62 | | | 12 | 10 | | |

perpendicular polarization. However, this second distance determination is not accurate, since such small differences of distance are always difficult to determine by standard EXAFS analysis. On the contrary, only one neighbor distance is necessary for the other samples. Finally, the simulated coordination numbers are very different between the thick Mn films and the SL's. It is between 5 and 7 for thick Mn films and around 12 for SL's.

This analysis consequently allows us to distinguish two different Mn structures in these samples. For relaxed thick Mn films, Mn is surrounded by neighbors at several distances around 2.35, 2.7, and 3 Å and the corresponding coordination numbers are small ($\leqslant 5$). This analysis is less clear in the case of unrelaxed thick Mn films, but the coordination numbers are also small ($\leqslant 7$). These results suggest that the Mn structure in thick films is probably close to the usual Mn$\alpha$, Mn$\beta$, or Laves phases structures. On the contrary, the large coordination numbers obtained in SL's suggest that the Mn structure is close to a fcc structure.

However, this analysis is not sufficient to clearly determine the Mn structures in these samples. Moreover, it does not show significant differences between relaxed and unrelaxed thick films, and between (111) and (001) SL's. Some differences can be, however, observed by RHEED, XRD, and EXAFS spectra. At this stage of investigation, it becomes necessary to apply the multiple scattering approach to EXAFS oscillations in order to go further.

### C. EXAFS oscillation calculations and comparison with experiments

*Relaxed thick Mn films*. We first know that these films are polycrystalline. Moreover, the calculated EXAFS spectrum for the Mn$\alpha$ structure (Fig. 1) and the experimental EXAFS spectra (Fig. 3) are similar. These two spectra are superimposed in Fig. 4. This demonstrates that the Mn films grown on (111) and (001) Ir surface relaxed to the Mn$\alpha$ polycrystalline phase. Moreover, this example shows the ability of the MS theory to account for the EXAFS oscillations of a complex structure like Mn$\alpha$, with 58 atoms in the primitive cell.

*(111) Mn/Ir superlattices.* The similarity between the calculated EXAFS oscillations assuming an fcc structure (Fig. 1) and the experimental EXAFS oscillations (Fig. 3) shows that the Mn structure is close to the fcc structure. However, we know that Mn is not in a cubic structure. Indeed, the fcc Mn parameter is equal to 3.73 Å at room temperature,[15] and the Ir parameter is equal to 3.84 Å. This means that the (111) fcc Mn plane is not pseudomorphic to the (111) fcc Ir plane. However, we have checked by RHEED that the Mn layers are pseudomorphic to the (111) Ir plane in (111) Mn/Ir SL's. We thus assume that the Mn fcc structure is strained by Ir. The out of plane parameter $a_\perp$ can be calculated using the elastic theory,[15] since

$$\varepsilon_{zz}=\frac{a_\perp}{a_\perp^0}-1=-\left(\frac{2\nu}{1-\nu}\right)\varepsilon_{xx}=\left(\frac{2\nu}{1-\nu}\right)\left(\frac{a_\parallel}{a_\parallel^0}-1\right), \qquad (1)$$

where $\varepsilon_{xx}$ and $\varepsilon_{zz}$ are the in- and out-of-plane strains, $\nu$ the Poisson ratio (taken equal to 0.3 here), and $a_\parallel^0$ and $a_\perp^0$ the in-plane and out-of-plane distances for the unstrained fcc Mn structure, i.e., $a_\parallel^0=d_{(110)}=2.638$ Å and $a_\perp^0=d_{(111)}=2.154$ Å. Using $a_\parallel=2.715$ Å, Eq. (1) gives $a_\perp=2.1$ Å, which is close to the value obtained by XRD (2.15 Å). This deformation leads to a trigonal structure (space group $R3m$) with $a=2.715$ Å and $c=3a_\perp=6.3$ Å. The details of the structure and the choice of the polarization axes are given in Table III. The calculated EXAFS spectra are actually in good agreement with the experimental ones, as shown in Fig. 4. However, some difference between the experimental and calculated $k\chi$(k) amplitudes is observed for perpendicular polarization. This discrepancy can be explained by stacking faults. Indeed, in the case of a fcc structure grown in the (111) direction, the contribution to EXAFS from up and down planes is small for the ∥ polarization. The EXAFS spectra performed with ∥ polarization are thus mostly sensitive to in-plane neighbours. Consequently, they are almost insensitive to the presence of stacking faults. On the contrary, the in-plane atom scattering does not contribute to EXAFS performed with ⊥ polarization. These EXAFS spectra are thus only sensitive to up and down atomic planes and are thus largely affected by stacking faults. This is consistent with our observations.

*(001) Mn/Ir superlattices.* The experimental EXAFS spectra performed with a ∥ polarization (Fig. 3) are again close to the EXAFS spectra calculated for an fcc structure. However, the structure of Mn layers is again not cubic. We thus assume that the Mn structure results from a deformation of the fcc structure as in the previous case. A tetragonal structure is now assumed. The in-plane parameter is also chosen equal to the (110) Ir parameter (2.715 Å). The elastic calculation [Eq. (1)] thus gives $a_\perp=d_{(002)}=1.87$ Å. The tetragonal structure is thus defined with $a=2.715$ Å and $c=2a_\perp=3.74$ Å. This value is now far from the result obtained by XRD ($a_\perp=1.8$ Å, i.e., $c=3.6$ Å). The EXAFS spectra are thus simulated using a tetragonal structure (space group I4/m mm) with $a=2.715$ Å and various $c$ (Table III). The best fit is obtained for $c=3.5\pm0.05$ Å (Fig. 4), in agreement with the value obtained by XRD measurements. Consequently, the elastic theory does not account for this result.

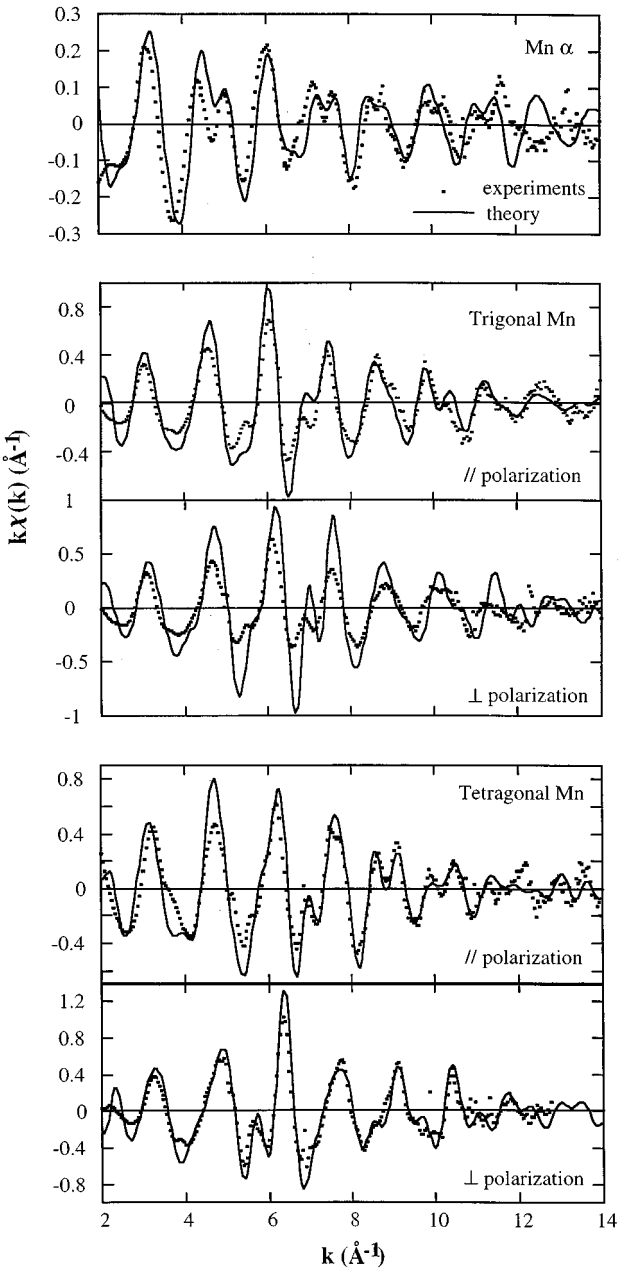


FIG. 4. Comparison between experimental and calculated EXAFS oscillations for a relaxed thick Mn film, a Mn/Ir(111) superlattice, and a Mn/Ir(001) superlattice.

This means that the Mn structure in (001) SL's does not correspond to a deformation of the fcc Mn structure. Indeed, this tetragonal structure is similar to the Mn tetragonal structure obtained in MnCu alloys extrapolated at zero Cu concentration.[16] Finally, it should be noted that the agreement between experimental and calculated $k\chi$(k) amplitudes is now good. This is not surprising since stacking faults are not favored in (001) direction.

*Unrelaxed thick Mn films.* It is not possible to fit the experimental EXAFS spectra measured on unrelaxed thick Mn films if a distorted fcc is considered. This is also the case if the Mn$\alpha$ structure is considered. Indeed, Heinrich *et al.*[5] proposed that Mn grows on Ru(0001) in a Laves phases like $Cu_2Mg$ or $Zn_2Mg$. This assumption allows them to explain the $(\sqrt{3}\times\sqrt{3})$ superstructure. Henry *et al.*[14] also explained RHEED experiments performed on Mn/Co(0001) by assuming the occurrence of the $Cu_2Mg$ structure. These Mn/Ru and Mn/Co systems are quite similar to the Mn/Ir(111) system since the $(\sqrt{3}\times\sqrt{3})$ superstructure is also observed. It was thus necessary to take these two possible structures into account. We know that the unrelaxed thick films are single crystalline and that the structure is cubic. Consequently, the Mn films cannot be in the $Zn_2Mg$ Laves phase. On the contrary, the $Cu_2Mg$ Laves phase is cubic. It is thus possible that Mn grows in this structure. However, the disagreement between calculated and experimental EXAFS spectra (see Figs. 1 and 3, respectively) definitely shows that the Mn structure is not a pure $Cu_2Mg$ Laves phase.

However, Henry *et al.* proposed that the Mn films are made of crystalline domains with the $Cu_2Mg$ and fcc structures. The EXAFS spectra were thus simulated assuming this coexistence. Again the experimental results cannot be explained by this assumption.

Finally, we know that thin Mn films grown on (111) Ir are in a strained fcc structure, and that relaxed thick Mn films are in the Mn$\alpha$ structure. It is thus natural to assume that both Mn$\alpha$ and fcc Mn structures coexist in unrelaxed thick Mn films. Assuming that the film is made of 50% of each phase, the EXAFS oscillations are actually well reproduced. This result can also be experimentally verified. In Fig. 5, a linear combination of experimental EXAFS spectra obtained on Mn$\alpha$ and distorted fcc Mn films is compared to the experimental EXAFS spectrum obtained on an unrelaxed thick Mn film. The striking similarities between these curves demonstrate that both structures coexist. This result is not surprising since the fcc Mn structure is present at the beginning of the growth. It simply shows that Mn epitaxially grows in the Mn$\alpha$ structure on top of this fcc Mn layer. The $(\sqrt{3}\times\sqrt{3})R30°$ superstructure is therefore due to this Mn$\alpha$ epitaxial growth. This scenario also explains the origin of the stacking faults in (111) Mn/Ir SL's. However, the fact that both phases coexist

TABLE III. Space groups, parameters, atom positions, and atomic volumes for the distorted fcc structures used to calculate the EXAFS spectra with the FEFF6 code (Ref. 8).

| Structure | Space group | Parameters (Å) | Atom positions and number of atom per cell | | | | Volume (Å$^3$/atom) |
|---|---|---|---|---|---|---|---|
| Trigonal | $R\bar{3}m$ | $a=2.715$<br>$c=6.3$ | 0 | 0 | 0 | (3) | 13.4 |
| Tetragonal | $I4/mmm$ | $a=2.715$<br>$c=3.5$ | 0 | 0 | 0 | (2) | 12.9 |

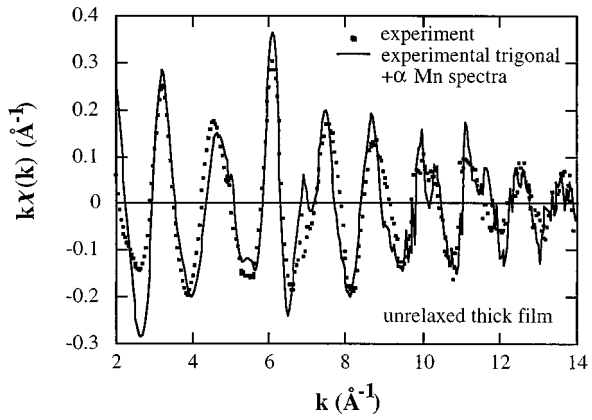


FIG. 5. Comparison of the experimental EXAFS oscillations of an unrelaxed thick Mn film with a linear combination of the experimental spectra obtained on a relaxed thick Mn film (50%) and a Mn/Ir(111) superlattice (50%).

with the same concentration is surprising. The details of the crystallographic arrangement of these two phases cannot be determined here.

## IV. CONCLUSIONS

It is well known that the standard analysis of EXAFS does not allow us to determine the structure of materials where the distances between first and second neighbors are close to one another. This is particularly well demonstrated here in the case of Mn. On the contrary, we show in this paper that the structure of Mn films grown on Ir can be determined with the help of multiple scattering theory. Indeed, the good agreement between the experimental and simulated EXAFS oscillations of the complex Mn$\alpha$ structure is particularly convincing. This allows us to propose the following scenario for the growth of Mn on (111) and (001) Ir.

On the (001) Ir lattice at 400 K, Mn grows in a tetragonal structure up to a critical thickness of around 100 Å. This structure does not result from a distortion of the standard fcc Mn structure. It seems to be a new Mn phase, similar to the Mn structure obtained in MnCu alloys with a Cu concentration close to zero. Above the critical thickness, the film entirely relaxes to the Mn$\alpha$ structure.

On the (111) Ir lattice at 400 K, Mn grows in a trigonal structure up to a critical thickness of three atomic planes. This trigonal structure arises from a distortion of the fcc Mn structure due to the Ir strain. Above this critical thickness, Mn epitaxially grows in both Mn$\alpha$ and fcc structures on top of this strained fcc phase. This growth regime operates up to a critical thickness of around 100 Å. However, the manner in which both phases simultaneously grow is not established in this paper. Above 100 Å, the entire Mn film relaxed towards the Mn$\alpha$ structure and the film is polycrystalline. When SL's are grown, the fcc structure can be grown up to critical thicknesses larger than three atomic planes, because of the Ir strain. However, the fcc structure is altered by stacking faults due to the beginning of the Mn$\alpha$ growth.

Finally, we clearly demonstrate that the $(\sqrt{3}\times\sqrt{3})R30°$ superstructure is not due to the growth of a Laves phase on (111) Ir. Indeed, this study allows us to assume that the Mn$\alpha$ and fcc Mn epitaxial growth is responsible for the occurrence of the $(\sqrt{3}\times\sqrt{3})R30°$ Mn structure. However, the atom arrangement which leads to this superstructure is difficult to establish.

[1] See, for instance, E. Bauer and J. H. Van der Merwe, Phys. Rev. B **33**, 3657 (1986); S. A. Barnett, in *Physics of Thin Films*, edited by M. H. Francombe and J. L. Vossen (Academic, San Diego, 1993), p. 1.

[2] M. Maurer, J. C. Ousset, M. F. Ravet, and M. Piecuch, Europhys. Lett. **9**, 803 (1989); S. Andrieu, M. Piecuch, and J. F. Bobo, Phys. Rev. B **46**, 4909 (1992); S. Andrieu, E. Snoeck, L. Hennet, H. Fischer, and M. Piecuch, Europhys. Lett. **26**, 189 (1994).

[3] S. Andrieu, F. Lahatra-Razafindramisa, E. Snoeck, H. Renevier, A. Barbara, J. M. Tonnerre, M. Brunel, and M. Piecuch, Phys. Rev. B **52**, 9938 (1995).

[4] See, for instance, F. Süss and U. Krey, J. Magn. Magn. Mater. **125**, 351 (1993).

[5] B. Heinrich, A. S. Arrott, C. Liu, and S. T. Purcell, J. Vac. Sci. Technol. A **5**, 1935 (1987).

[6] L. Nevot and M. Piecuch, Mater. Sci. Forum **59-60**, 93 (1990).

[7] A. Traverse, S. Pizzini, S. Andrieu, A. Fontaine, and M. Piecuch, Surf. Sci. **319**, 131 (1994).

[8] S. I. Zabinsky, J. J. Rehr, A. Andukinov, R. C. Albers, and M. J. Eller, Phys. Rev. B **52**, 2995 (1995).

[9] H. M. Fischer, thesis, University of Nancy, France, 1995.

[10] H. M. Fischer, H. E. Fischer, M. Bessiere, J. F. Bobo, O. Lenoble, S. Andrieu, and M. Piecuch, in *Structure and Properties of Multilayered Thin Films*, edited by Tai D. Nguyen *et al.*, MRS Symposia Proceeding, No. 382 (Materials Research Society, Pittsburgh, 1995), p. 339.

[11] J. Mimault, J. J. Faix, T. Girardeau M. Jaouen, and G. Tourillon, Meas. Sci. Technol. **5**, 482 (1994).

[12] See, for instance, A. Michalowizc, *Logiciels pour la Chimie* (Société Française de Chimie, Paris, 1991), Vol. 102.

[13] A. G. McKale, B. W. Veal, A. P. Paulikas, S. K. Chan, and G. S. Knapp, J. Am. Chem. Soc. **110**, 3763 (1988).

[14] Y. Henry, V. Pierron-Bohnes, P. Vennègues, and K. Ounadjela, J. Appl. Phys. **76**, 2817 (1994); K. Ounadjela, P. Vennègues, Y. Henry, A. Michel, V. Pierron-Bohnes, and J. Arabski, Phys. Rev. B **49**, 8561 (1994).

[15] D. Tian, S. C. Wu, F. Jona, and P. M. Marcus, Solid State Commun. **70**, 199 (1989).

[16] *Pearson's Handbook of Crystallographic Data for Intermetallic Phases*, edited by P. Villars and L. D. Catvert (American Society for Metals, Metals Park, OH, 1985), Vol. 3, p. 2710.